

What coil has the highest Q ?

A. Rikhter and M. M. Fogler

Department of Physics, University of California San Diego, 9500 Gilman Drive, La Jolla, California 92093, USA

(Dated: 27 March 2022)

The geometry of an inductor made of a long thin wire and having the highest possible Q -factor is found by numerical optimization. As frequency increases, the Q -factor first grows linearly and then according to a square-root law, while the cross-section of the optimal coil evolves from near-circular to sickle-shaped.

Introduction.—Given a piece of wire, how can one wind it into a coil of the maximum possible Q -factor? While previously this question has been treated almost exclusively in the context of radio engineering,^{1,2} in this work we address it as a problem in mathematical physics. To constrain the size of the coil, we have the following geometric parameters fixed: the total wire length W , the conducting core diameter d_i , and the effective outer diameter d . We define d in terms of the maximum possible wire density $n_2 \equiv (\pi d^2/4)^{-1}$ per unit area. Thus, for the hexagonal closed packing of round wires, d is $(12/\pi^2)^{1/4} = 1.050$ times the actual outer diameter. The current is taken to be $I = e^{-i\omega t}$. We consider only frequencies ω much smaller than the self-resonance frequency $\omega_r \sim c/W$ of the coil, allowing us to neglect the capacitance term. With these simplifying assumptions, current is uniform along the wire, and the Q -factor can be defined as the ratio of the imaginary and real parts of the complex impedance $Z = R + i\omega L$:

$$Q(\omega) = \frac{\text{Im } Z}{\text{Re } Z} = \frac{\omega L(\omega)}{R(\omega)}. \quad (1)$$

Because of induced eddy currents, $R(\omega)$ is coil-shape dependent, so that the competition between the inductance and the losses poses a nontrivial optimization problem for $Q(\omega)$.

Our electrodynamic problem has roots in a magnetostatic problem first studied by Gauss.³ Specifically, in the limit $\omega \rightarrow 0$, the effective resistance R approaches the dc resistance $R(0) = 4W/(\pi\sigma d_i^2)$, where σ is the core conductivity, so that maximizing Q is equivalent to maximizing L . Gauss assumed that the coil of the highest L under the aforesaid constraints is a toroidally wound solenoid with a nearly circular cross-section, Fig. 1(a). Later, Maxwell⁴ revisited the problem and treated a more practical case of a square cross-section, Fig. 1(b). Maxwell's analysis was improved by Rosa and Grover.⁵ Building on their work, Brooks proposed that the mean radius of the optimal coil is approximately $3/2$ of the side of the square.⁶ The inductance of this coil is $0.656L_c$, where

$$L_c = \frac{\mu_0}{4\pi} \frac{W^{5/3}}{d^{2/3}}. \quad (2)$$

Optimization of inductors with nonmagnetic cores became topical again in the 1970's when toroidal coils (wound in the poloidal direction) were brought in a wider use in plasma physics and energy storage research.

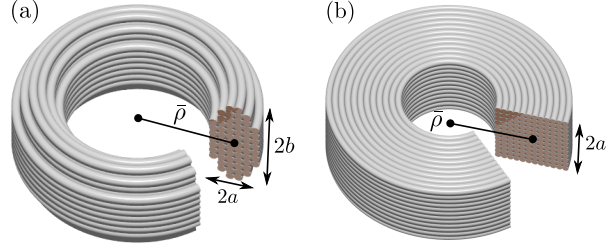


FIG. 1. Schematics of multi-layer coils with (a) elliptic and (b) square cross-sections.

The case of a single-layer toroid was solved by Shafrazenov.^{7,8} Multilayer coils were studied by Murgatroyd^{9,10} who found that the inductance of the optimal toroid is $0.29L_c$. The reduction compared to the Brooks coil is presumably because the toroid generates no stray magnetic field. Murgatroyd reviewed the $5/3$ power-law of Eq. (2) and other properties of optimal inductors in his excellent summary.⁹ For example, the characteristic size of such inductors is set by

$$\rho_c = \frac{1}{2}(Wd^2)^{1/3}. \quad (3)$$

Below we derive scaling laws for finite- ω optimal inductors, in terms of two additional characteristic scales:

$$\omega_c \equiv \frac{8\pi}{Q_c \mu_0 \sigma d_i^4}, \quad Q_c \equiv \frac{2\rho_c}{d_i}. \quad (4)$$

The former is the frequency at which the eddy-current losses become comparable with the dc Ohmic ones, the latter is the order of magnitude of the Q -factor at ω_c .

Low frequencies.—We begin with answering Gauss' question about the dc inductance. It was posed by him 150 years ago but apparently has not been settled yet. Gauss' calculation can be summarized as follows. An estimate of L is provided by the approximate formula⁴

$$L = \mu_0 N^2 \bar{\rho} \left[\ln \left(\frac{8\bar{\rho}}{\text{GMD}} \right) - 2 \right], \quad (5)$$

where N is the total number of turns in the coil and $\bar{\rho}$ is their mean radius. Note that $2\pi\bar{\rho}N = W$. Parameter GMD is the geometric mean distance. In the continuum limit, appropriate for large N , it is defined via

$$\ln(\text{GMD}) = \frac{1}{A^2} \iint \ln |\mathbf{r} - \mathbf{r}'| d^2r d^2r', \quad (6)$$

where positions $\mathbf{r} = (\rho, z)$, $\mathbf{r}' = (\rho', z')$ vary over the cross-section of the coil, of the area $A = N/n_2$. According to Eq. (5), to maximize L for a given N (or $\bar{\rho}$) we need to minimize GMD at fixed A . It can be proven¹¹ that the solution is a circle of radius $a = \sqrt{A/\pi}$ whose GMD is⁵ $e^{-1/4}a$. Minimizing L with respect to $\bar{\rho}/a$, Gauss obtained $\bar{\rho}/a = e^{13/4}/8 = 3.22$. Such a mean-radius to half-height ratio is noticeably different from either 3.7 or 3 advocated by, respectively, Maxwell and Brooks, see Fig. 2(a), suggesting that this method is too crude to reveal the true optimal coil geometry.

To glean a more accurate answer, we tackled the problem numerically. We expressed the inductance and the wire-length constraint in the form of integrals,

$$L = \iint n(\mathbf{r}) M(\mathbf{r}, \mathbf{r}') n(\mathbf{r}') d^2 r d^2 r', \quad (7)$$

$$W = \int n(\mathbf{r}) 2\pi\rho d^2 r, \quad (8)$$

where $0 \leq n(\mathbf{r}) \leq n_2$ is the number of turns per unit area at position \mathbf{r} . Function $M(\mathbf{r}, \mathbf{r}')$, given by

$$M(\mathbf{r}, \mathbf{r}') = \mu_0 \sqrt{\frac{\rho\rho'}{m}} [(2-m)K(m) - 2E(m)], \quad (9)$$

$$m = \frac{1}{1+k^2}, \quad k = \frac{|\mathbf{r} - \mathbf{r}'|}{\sqrt{4\rho\rho'}}$$

is the mutual inductance of co-axial rings⁵ piercing the cross-section at \mathbf{r} and \mathbf{r}' ; $K(m)$ and $E(m)$ are the complete elliptic integrals. We approximated the integrals in Eqs. (7), (8) by sums over a finite two-dimensional grid and performed the constrained maximization of L

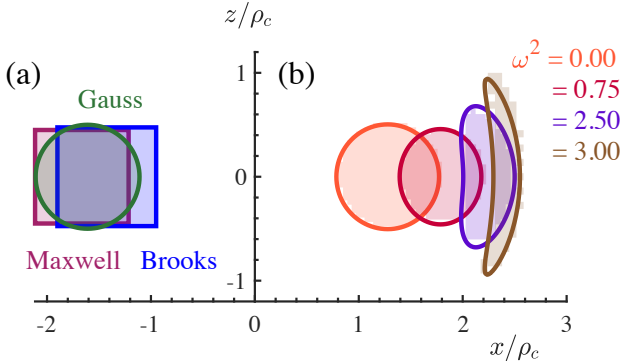


FIG. 2. Cross-sections of the optimal coils. (a) Designs proposed by Gauss,³ Maxwell,⁴ and Brooks.⁶ (b) Results obtained in this work. The cross-section evolves from near-circular to elliptic to sickle-shaped as ω increases. The shading represent the local wire density $n(\mathbf{r})$ computed on a 30×30 grid. The curves serve as guides to the eye. The wire density is seen to switch from 0 to n_2 with few or no intermediate values. The numbers on the axes are x and z coordinates in units of ρ_c . The legend indicates the magnitudes of $(\omega/\omega_c)^2$.

numerically. The outcome of these calculation is as follows. The mean radius of the optimal coil is $\bar{\rho} = 1.28\rho_c$. The cross-section of the coil is not a circle; it is better approximated by an ellipse of dimensions

$$\xi_1 \equiv \frac{\bar{\rho}}{a} = 2.54, \quad \xi_2 \equiv \frac{\bar{\rho}}{b} = 2.61, \quad (10)$$

represented by the curve labeled $\omega^2 = 0$ in Fig. 2(b). The cross-section is fully packed, so that

$$n(\mathbf{r}) = n_2 \Theta \left(1 - \frac{(\rho - \bar{\rho})^2}{a^2} - \frac{z^2}{b^2} \right), \quad (11)$$

where $\Theta(x)$ is the unit step-function. Finally, the coil inductance is

$$L = 0.663L_c, \quad (12)$$

which is 1% larger than that of the Brooks coil.

Encouraged by the simplicity of these results, we re-derived them as follows. We started with the expansion⁵

$$M(\mathbf{r}, \mathbf{r}') \simeq \mu_0 \sqrt{\rho\rho'} \left[\left(1 + \frac{3k^2}{4} \right) \ln \frac{4}{k} - 2 - \frac{3k^2}{4} \right], \quad (13)$$

valid for $k \ll 1$ [Eq. (9)], and evaluated the integral in Eq. (7) analytically for the elliptic cross-section defined by Eq. (11). The result can be written as

$$L = \mu_0 N^2 \bar{\rho} \Lambda, \quad (14)$$

$$\Lambda = \left(1 + \frac{1}{32} \frac{\xi_2^2 + 3\xi_1^2}{\xi_1^2 \xi_2^2} \right) \ln \left(\frac{16\xi_1 \xi_2}{\xi_1 + \xi_2} \right) - \frac{7}{4} + \frac{7}{96} \frac{1}{\xi_1^2} + \frac{1}{32} \frac{\xi_2^2 - 3\xi_1^2}{\xi_1^2 \xi_2^2} \frac{\xi_1}{\xi_1 + \xi_2}, \quad (15)$$

which is a generalization of Rayleigh's formula¹² for the $b = a$ case and a key improvement over Eq. (5). Using this formula for L and another one, $W = \pi a b \bar{\rho} n_2$, for the length constraint, we were able to easily solve for the optimal ξ_1 , ξ_2 numerically, reproducing Eq. (10).

Returning to the Q -factor, we rewrite Eq. (1) in terms of our characteristic scales L_c , Q_c , ω_c :

$$Q = \frac{\pi}{2} \frac{\omega}{\omega_c} \frac{L/L_c}{1 + F(\omega)} Q_c, \quad (16)$$

where we introduced the loss enhancement factor

$$F(\omega) \equiv \frac{R(\omega)}{R(0)} - 1. \quad (17)$$

Below we show that at low frequencies $\omega \ll \omega_c$, the loss factor behaves as

$$F(\omega) = 0.305 \frac{\omega^2}{\omega_c^2}. \quad (18)$$

At such frequencies, $F \ll 1$ is negligible, L is virtually unchanged from the dc value, and so the Q -factor is linear in ω :

$$\frac{Q}{Q_c} = 1.04 \frac{\omega}{\omega_c}, \quad \omega \ll \omega_c, \quad (19)$$

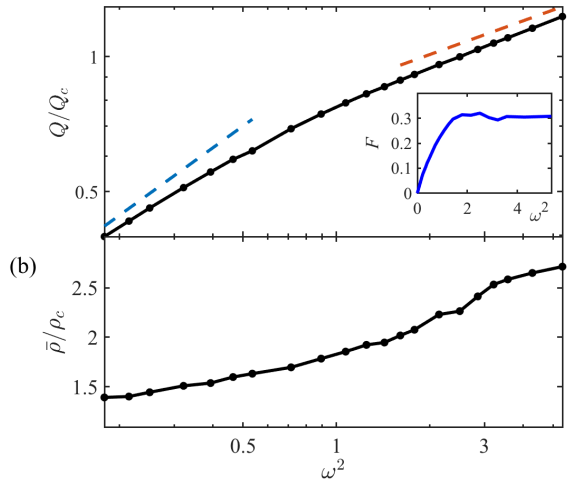


FIG. 3. (a) Q -factor of the optimal coil as a function of ω^2/ω_c^2 . The connected dots are our numerical results. The two dashed lines indicate the expected low- and intermediate-frequency scaling. Inset: loss factor F vs. ω^2/ω_c^2 . (b) Mean radius $\bar{\rho}$ of the coil in units of ρ_c as a function of ω^2/ω_c^2 .

see Fig. 3.

Proximity effect losses.—The finite-frequency losses in coils are traditionally attributed to the combination of the skin and proximity effects.¹³ The latter, due to the collective field $\mathbf{H}(\mathbf{r})$ of all the turns of the wire, dominates in multi-layer coils of interest to us if ω is not too high, such that $\delta \gg d_i$, where

$$\delta(\omega) = \sqrt{\frac{2}{\mu_0 \omega \sigma}} \quad (20)$$

is the skin depth. Under the stated condition of weak skin effect, the loss factor takes the form

$$F(\omega) = \frac{\pi^2}{64W} \frac{d_i^6}{\delta^4} \int \mathbf{H}^2(\mathbf{r}) n(\mathbf{r}) 2\pi\rho d^2r \quad (21)$$

where \mathbf{H} , equal to the curl of a vector potential, is

$$\mathbf{H}(\mathbf{r}) = \frac{1}{2\pi\mu_0\rho} (\hat{\mathbf{z}}\partial_\rho - \hat{\boldsymbol{\rho}}\partial_z) \int M(\mathbf{r}, \mathbf{r}') n(\mathbf{r}') d^2r'. \quad (22)$$

In general, these expressions have to be evaluated numerically. However, we can estimate F analytically for a coil with the elliptic cross-section, Eq. (11). Retaining only the leading-order terms in $k \sim \max(a, b)/\bar{\rho} \ll 1$ in Eq. (13), we find

$$\mathbf{H}(\mathbf{r}) = \frac{n_2}{a+b} [az\hat{\boldsymbol{\rho}} - (\rho - \bar{\rho})b\hat{\mathbf{z}}]. \quad (23)$$

Substituting this into Eq. (21), we get

$$F = \frac{1}{8} \left(\frac{d_i^3}{\delta^2 d^2} \frac{ab}{a+b} \right)^2 = \frac{\pi^2}{2} \frac{\omega^2}{\omega_c^2} \left(\frac{1}{\rho_c} \frac{ab}{a+b} \right)^2, \quad (24)$$

which is a generalization of Howe's formula for a multi-stranded round wire.¹⁴ Finally, using Eqs. (3) and (10), we arrive at Eq. (18). At the border of its validity, $\omega \approx \omega_c$, that equation predicts $F \approx 0.3$ assuming the wire is long enough so that $\delta/d_i \approx 0.2(W/d)^{1/6} \gg 1$.

Intermediate frequencies.—At $\omega \gg \omega_c$ the competition between inductance and proximity losses is expected to cause flattening of the cross-section of the optimal coil. We confirmed this hypothesis by numerical simulations based on Eqs. (7), (8), (21), and (22). Our results for a few representative ω are shown in Fig. 2(b). As frequency increases, the cross-section first becomes oval and then sickle-shaped. Figure 3 presents the Q -factor and the mean radius $\bar{\rho}$ obtained from these simulations. The plot in the main panel of Fig. 3(a) suggests that the linear scaling of $Q(\omega)$ changes to a square-root law above the frequency ω_c as the cross-section begins to flatten and bend. The inset of Fig. 3(a) illustrates that the loss factor grows as predicted by Eq. (18) at $\omega/\omega_c < 1$ but reaches a constant $F \approx 0.3$ at $\omega/\omega_c > 1$.

We can shed light on the observed $\omega/\omega_c > 1$ behaviors using our elliptical cross-section model. Assuming $a \ll b$, we derive the following analytical expressions for a and b in terms of dimensionless parameters $\xi_2 = \bar{\rho}/b$ and F :

$$\frac{a}{\rho_c} = \sqrt{\frac{F}{2\pi^2}} \frac{\omega_c}{\omega}, \quad \frac{b}{\rho_c} = \sqrt{\frac{1}{\pi\xi_2} \frac{\rho_c}{a}}. \quad (25)$$

They entail that Q at a given ω has the scaling form

$$Q(\xi_2, F) = \frac{F^{1/4}}{1+F} q(\xi_2). \quad (26)$$

Hence, Q at fixed ξ_2 reaches its maximum at $F = 1/3$, which is close to our numerical result. Freezing F at $1/3$ and maximizing Q with respect to ξ_2 , we arrived at

$$\frac{Q}{Q_c} = 0.85 \sqrt{\frac{\omega}{\omega_c}}, \quad \frac{\bar{\rho}}{\rho_c} = 1.6 \sqrt{\frac{\omega}{\omega_c}}, \quad (27)$$

$$\frac{a}{\rho_c} = 0.26 \frac{\omega_c}{\omega}, \quad \xi_2 = 2.13. \quad (28)$$

The first equation in Eq. (27), represented by the upper dashed line in Fig. 3(a), is within 10% from the simulation results. The second equation in Eq. (27), has a similar level of agreement with the data in Fig. 3(b). This is satisfactory considering that ω/ω_c is not truly large and that our analytical model is oversimplified.

High frequencies.—From now on we focus on the practical case of densely packed, thinly insulated wires, $d_i \approx d$. Per Eqs. (20) and (25), at frequency $\omega_s = \omega_c Q_c / (2\pi) \gg \omega_c$ both the width $2a$ of the thickest part of the winding and the skin depth δ become of the order of d . This implies that at $\omega \gg \omega_s$ the optimal coil is (i) single-layered and (ii) strongly affected by the skin effect. In view of the former, we can fully specify the cross-sectional shape of the coil by a function $\rho(z)$ and replace Eqs. (7) and (8)

by

$$L = n_1^2 \iint M(\mathbf{r}, \mathbf{r}') \sqrt{1 + \rho'^2(z)} \sqrt{1 + \rho'^2(z')} dz dz', \quad (29)$$

$$W = n_1 \int 2\pi \rho(z) \sqrt{1 + \rho'^2(z)} dz \quad (30)$$

with $n_1 \sim 1/d$ being the number of turns per unit arc length of the cross-section. Equation (21) gets modified as well. As first shown by Rayleigh,¹⁵ a single straight round wire is characterized by the loss factor $F_s = d_i/(4\delta) \gg 1$, due to confinement of the current to a δ -thick skin layer at the conductor surface. In a coil or in a bunch of parallel wires, inter-wire interactions cause further nonuniformity of the current in the skin layer. As a result, the loss factor increases beyond Rayleigh's F_s :

$$\frac{F}{F_s} = \lambda + \frac{d_i^2 n_1}{8} \int [f H_{\parallel}^2(z) + g H_{\perp}^2(z)] 2\pi \rho dz, \quad (31)$$

where $H_{\parallel}(z)$ and $H_{\perp}(z)$ are the components of $\mathbf{H}(\mathbf{r})$ parallel and perpendicular to the layer,

$$H_{\parallel}(z) = \frac{H_{\rho} \rho' + H_z}{\sqrt{1 + \rho'^2}}, \quad H_{\perp}(z) = \frac{H_{\rho} - H_z \rho'}{\sqrt{1 + \rho'^2}}. \quad (32)$$

The dimensionless coefficients λ , f , and g introduced by Butterworth¹³ depend on the wire packing density $n_1 d_i$ and have to be calculated numerically.¹⁶ The optimization of Q using the entire set of these complicated equations appears to be challenging, so we have not attempted it. On the other hand, the solution for $\rho(z)$ we present below is a nearly constant function. For such functions the loss factor F should be weakly shape dependent, in which case to maximize Q it is sufficient to maximize L alone. We accomplished the latter numerically using Eqs. (29) and (30), in which we additionally dropped the $\sqrt{1 + \rho'^2}$ factors. The optimal solenoid shape we found is slightly convex, as depicted schematically in Fig. 4, with the aspect ratio $\xi = \bar{\rho}/l = 2.20$ and curvature $0.0024/l$. Note that ξ is numerically close to ξ_2 in the intermediate frequency regime, Eq. (28). Substituting the obtained L into Eq. (16), we got

$$\frac{Q}{Q_c} = \frac{2.34}{F/F_s} \sqrt{\frac{\omega}{\omega_c}}, \quad \omega \gg \omega_s, \quad (33)$$

which is similar to Eq. (27) but has a different coefficient. This high-frequency behavior is actually well-known in radio engineering.^{1,2}

In an effort to rederive these results more simply, we considered a family of constant-radius solenoids whose inductance is given by Lorenz's formula⁵

$$L = \frac{8}{3} \mu_0 n_1^2 \rho^3 \left[\frac{2m-1}{m\sqrt{m}} E(m) + \frac{1-m}{m\sqrt{m}} K(m) - 1 \right], \quad (34)$$

where $m = \rho^2/(\rho^2 + l^2)$. As seen in Fig. 4, the maximization of this L (under the constraint $4\pi\rho ln_1 = W$) gives

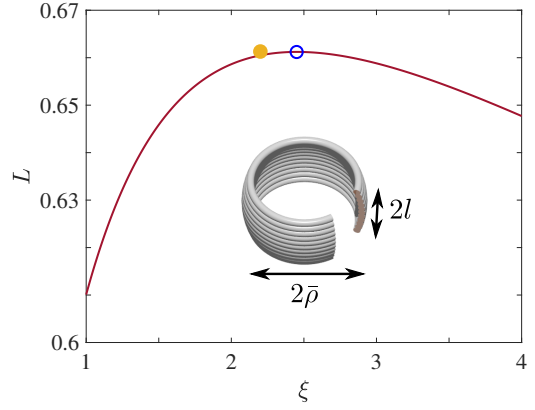


FIG. 4. Inductance L of a constant-radius single-layer coil as a function of $\xi = \bar{\rho}/l$. The open dot labels the maximum on the curve. The filled dot shows the true optimum. L is in units of $\mu_0 W^{3/2}/(2\pi\sqrt{d})$. Inset: definitions of $\bar{\rho}$ and l .

$L = 0.661 \mu_0 W^{3/2}/(2\pi\sqrt{d})$, in agreement with Murgatroyd.⁹ This is only $\sim 1\%$ lower than the true optimum.

Yet the best aspect ratio for the constant-radius solenoid proves to be 2.46, a 13% larger than for our optimal coil.

Discussion.—In this work we studied theoretically the highest possible Q -factor of an inductor wound from a given piece of wire. Real inductors used in various practical applications^{17–19} are made under numerous additional constraints, such as minimal cost or ease of manufacturing. Depending on the application, a multitude of related optimization problems arises. Our calculation provides a fundamental upper bound on Q and its scaling with wire length, diameter, and frequency. At the highest frequencies we considered, $Q(\omega)$ grows according to the square-root law. Unless the conductivity σ of the wire material is very low, we expect this law to persist up to the self-resonance frequency $\omega_r \sim c/W$ of the coil where the ultimate limit of Q is achieved. If σ is small, then radiation losses neglected in our model would need to be considered before ω_r is reached. This problem may be relevant for optimizing metamaterial resonators, and so it could be an interesting topic for future research.

Acknowledgments.—This work was supported by The Office of Naval Research under grant N00014-18-1-2722 and by General ElectroDynamics International, Inc. We thank Yu. A. Dreizin for discussions that inspired this study and also B. I. Shklovskii and E. Yablonovitch for comments on the manuscript.

¹R. G. Medhurst, *Wireless Eng.* **24**, 35 (1947).

²R. G. Medhurst, *Wireless Eng.* **24**, 82 (1947).

³C. F. Gauss, *Werke*, Vol. 5 (Cambridge University Press, Cambridge, 2011) (first published in 1867).

⁴J. C. Maxwell, *Treatise on Electricity and Magnetism*, 3rd ed., Vol. 2 (Dover, New York, 1954), article 706.

⁵E. B. Rosa and F. W. Grover, *Bulletin of the Bureau of Standards* **8**, 1 (1912).

⁶H. B. Brooks, *Bureau of Standards Journal of Research* **7**, 298 (1931).

⁷V. D. Shafranov, Sov. Phys. - Tech. Phys. **17**, 1433 (1973).

⁸S. L. Gralnick and F. H. Tenney, J. Appl. Phys. **47**, 2710 (1976).

⁹P. N. Murgatroyd, IEEE Trans. Mag. **25**, 2670 (1989).

¹⁰P. N. Murgatroyd and D. P. Eastaugh, IEE Proc. Electric Power Appl. **147**, 75 (2000).

¹¹G. Pólya and G. Szegő, *Isoperimetric inequalities in mathematical physics*, Annals of Mathematics Studies, Vol. 27 (Princeton University Press, Princeton, 1951).

¹²L. Rayleigh, Proc. Roy. Soc. A **86**, 562 (1912).

¹³S. Butterworth, Proc. Roy. Soc. A **107**, 693 (1925).

¹⁴G. W. O. Howe, Proc. Roy. Soc. A **93**, 468 (1917).

¹⁵L. Rayleigh, The London, Edinburgh, and Dublin Philosophical Magazine and Journal of Science **21**, 381 (1886).

¹⁶G. S. Smith, J. Appl. Phys. **43**, 2196 (1972).

¹⁷J. N. Burghartz and B. Rejaei, IEEE Trans. Electron Dev. **50**, 718 (2003).

¹⁸S. Tumanski, Meas. Sci. Tech. **18**, R31 (2007).

¹⁹A. Karalis, J. D. Joannopoulos, and M. Soljačić, Ann. Phys. **323**, 34 (2008).